ASM | Antimicrobial Agents and Chemotherapy

| Antimicrobial Chemotherapy | Short Form

PER-14, a β-lactamase variant with reduced sensitivity to avibactam and relebactam

Melina Ruggiero,[1,2] Melina García Alonso,[1] Salvador I. Drusin,[3,4] Roque Figueroa-Espinosa,[1] Ivan Jackson Briceño Muñoz,[1] Robert A. Bonomo,[5,6,7,8,9,10,11,12] Gabriel Gutkind,[1,2] José Di Conza,[1,2] Diego M. Moreno,[3,4] Pablo Power[1,2]

AUTHOR AFFILIATIONS See affiliation list on p. 5.

ABSTRACT PER-1-producing *Pseudomonas* and *Acinetobacter* and PER-2-producing *Enterobacterales*, respectively, are increasingly difficult to treat due to combined resistance to antibiotics like ceftazidime, cefiderocol, and ceftazidime/aztreonam-avibactam, among others. PER-14 differs from PER-2 by an S130T substitution. Through combined functional and *in silico* analyses, we demonstrated that PER-14 is resistant to avibactam and relebactam inhibition while retaining an extended-spectrum activity and the ability to hydrolyze cefiderocol, as the S130T substitution affects the proper binding of the DBOs.

KEYWORDS *Pararheinheimera*, ceftazidime/avibactam, ceftazidimase, ESBL, diazabicyclooctane, aztreonam/relebactam

The PER family of class A serine β-lactamases has been likely recruited from different environmental *Pararheinheimera* species (1). From the 18 recognized variants (http://bldb.eu/BLDB.php?prot=A#PER), PER-1 and PER-2 are the most frequently reported in *Pseudomonas*/*Acinetobacter* and *Enterobacterales*, respectively (2).

The diazabicyclooctane inhibitors (DBOs) avibactam (AVI) and relebactam (REL) are currently employed for the treatment of infections caused by multidrug-resistant gram-negative bacteria (3). Although AVI and REL exhibit potent activity against most serine-β-lactamases, PER β-lactamases are associated with resistance to ceftazidime-avibactam and aztreonam-avibactam (ATM-AVI) in *Pseudomonas* spp. and *Enterobacterales* (4–7). In previous studies, the efficacy of AVI against PER-2 was demonstrated to be lower compared to other class A β-lactamases (8, 9). Additionally, the co-production of NDM and PER β-lactamases is associated with decreased susceptibility or resistance to cefiderocol (FDC) in *Pseudomonas aeruginosa*, *Providencia rettgeri*, and *Acinetobacter baumannii* (5, 10, 11). PER-2 was demonstrated to hydrolyze FDC with catalytic efficiency values equivalent to NDM-1 (12). The INFORM global surveillance study (2012–2017) identified a *Raoultella ornithinolytica* isolate from Argentina with an ATM-AVI MIC of 16/4 µg/mL, carrying a novel PER variant assigned as PER-14 (4).

This study aims to provide a phenotypic and kinetic characterization of PER-14. bla_{PER-14} differs from bla_{PER-2} by a single nucleotide resulting in an S130T substitution, which was previously linked to increased AVI resistance in PER-4 (7, 13). In class A β-lactamases, S130 has an important role during acylation, as it participates in proton shuttling, substrate recognition, and inhibitor binding (14, 15).

The bla_{PER-14} and $bla_{PER-2/S130G}$ genes were generated by site-directed mutagenesis from bla_{PER-2} using a PCR-based overlap extension protocol (16); the PER-2^{S130G} variant was designed to better assess the impact of substitutions at amino acids in position 130. *Escherichia coli* TOP10F′ was transformed with pUC57-kan constructions containing the cloned bla_{PER} genes, and the MICs were determined according to CLSI guidelines (17).

Editor Laurent Poirel, University of Fribourg, Fribourg, Switzerland

Address correspondence to Pablo Power, ppower@ffyb.uba.ar.

The authors declare no conflict of interest.

See the funding table on p. 6.

Received 12 March 2026
Accepted 30 June 2026
Published 21 July 2026

Copyright © 2026 Ruggiero et al. This is an open-access article distributed under the terms of the Creative Commons Attribution 4.0 International license.

The MICs for tested antibiotics were similar for both PER-14- and PER-2-producing clones except for ATM, where the MIC decreased by four dilutions in the PER-14-producing clone (Table 1). AVI and REL failed to reduce MICs of CAZ or ATM in the PER-14-producing strain, although they were efficient in reducing the MICs by up to nine dilutions in the PER-2-producing clone. Sulbactam and clavulanic acid effectively reduced MICs for ampicillin (AM) and ATM, respectively, in both PER-2- and PER-14-producing clones (Table 1). For PER-2^{S130G}, a similar MIC value was obtained only for AM. All cephalosporins and ATM exhibited considerably lower MIC values, indicating the inability of this variant to efficiently hydrolyze these substrates. Increased susceptibility to FDC was also observed in the PER-2^{S130G} variant.

PER-14 and PER-2^{S130G} production and purification, as well as the evaluation of AVI and REL inhibition using 100 µM nitrocefin (NCF) as a reporter substrate, were performed as previously described (9). As the catalytic behavior of the enzymes remains reproducible, we used this feature, combined with assessment of protein purity by SDS-PAGE, as adequate criteria to estimate protein integrity and purity.

Kinetic data supported antimicrobial susceptibility behavior (Table 2). Catalytic efficiencies (k_{cat}/K_m) were comparable between PER-2 and PER-14 for all tested antibiotics. We previously demonstrated that PER-2 is inhibited by AVI with acylation rates reminiscent of values observed for class C and D β-lactamases (k_2/K of ≅10^3 M^{-1} s^{-1}) but lower than other class A β-lactamases (k_2/K of ≅10^4 to 10^5 M^{-1} s^{-1}) (8, 9). When comparing the steady-state inhibition of PER-14 and PER-2 by DBOs (Table 3), the $K_{i\ app}$ of AVI was 37-fold higher for PER-14, while the k_2/K decreased by approximately 880-fold, indicating that in PER-14, both the binding and the acylation step are compromised. For REL, the $K_{i\ app}$ was 200-fold higher for PER-14, while the k_2/K was reduced by approximately 3,200-fold. The deacylation rate constant (k_{off}) for the PER-2/AVI and PER-2/REL was equivalent (0.0004 and 0.0002 s^{-1}, respectively) and comparable to other class A β-lactamases (8). We were unable to determine the k_{off} for PER-14, mainly because of very high K_m values (low affinity) and/or low k_2/K constants (slow acylation rate).

For PER-2^{S130G}, similar k_{cat}/K_m values were only obtained for the hydrolysis of AM and NCF (Table 2), although a competitive inhibition by NCF product was observed (19). For the rest of the antibiotics, the k_{cat}/K_m decreased considerably by a factor higher than 10, mainly due to a decrease in the k_{cat}. For FDC, the catalytic efficiency of this variant was up to 150 times lower than PER-2 and PER-14, in agreement with the observed decrease in the MIC. AVI and REL were also unable to efficiently inhibit the enzyme (Table 1), and since the enzyme cannot properly hydrolyze CAZ or ATM either, a combination of these inhibitors and antibiotics would be effective for PER-2^{S130G}. These observations are consistent with isolates producing other class A β-lactamases (i.e., KPC-2 or CTX-M-15), where the S130G substitution confers AVI resistance, but the enzymes also lose the ability to hydrolyze cephalosporins (21, 22).

Molecular dynamics (MD) simulations and docking studies were performed to gain structural insight into the reduced susceptibility of PER-14 to DBO inhibitors, according to Drusin et al. (23). The experimental details are provided as Text S1 in the supplemental material.

The MD simulations revealed a marked difference between PER-2 and PER-14 in the conformational behavior of residue 130. In PER-2, S130 fluctuated between two preferred orientations: one in which the hydroxyl group points toward the inhibitor-binding

TABLE 1 MIC values of β-lactam antibiotics and combinations with β-lactamase inhibitors for PER-14 and PER-2-producing clones[a]

E. coli TOP10F′	MIC (µg/mL)										
	AM	AMS	CF	CRO	CAZ	CAZ-AVI	FEP	FDC	ATM	ATM-AVI	ATM-REL	ATM-CLA
PER-2/pUC57-kan	>512	16/8	256	128	512	2/4	16	0.5	1,024	2/4	1/4	0.25/4
PER-14/pUC57-kan	256	64/32	256	64	128	128/4	8	0.5	64	64/4	32/4	0.25/4
PER-2^{S130G}/pUC57-kan	512	16/8	8	0.25	16	4/4	0.5	0.03	8	2/4	8/4	0.5/4
pUC57-kan	4	4/2	4	0.06	0.25	0.25/4	0.06	0.03	0.25	0.25/4	0.25/4	0.25/4

[a]AM, ampicillin; AMS, ampicillin-sulbactam; ATM, aztreonam; ATM-AVI, aztreonam-avibactam; ATM-CLA, aztreonam-clavulanate; ATM-REL, aztreonam-relebactam; CAZ, ceftazidime; CAZ-AVI, ceftazidime-avibactam; CF, cephalothin; CRO, ceftriaxone; FEP, cefepime; FDC, cefiderocol.

TABLE 2 Steady-state kinetic parameters for PER-14, PER-2^{S130G}, and PER-2 against β-lactam antibiotics[e]

Antibiotic	PER-14 (PER-2^{S130T})			PER-2^{S130G}			PER-2[c]		
	K_m (μM)	k_{cat} (s^{-1})	k_{cat}/K_m ($\mu M^{-1}\cdot s^{-1}$)	K_m (μM)	k_{cat} (s^{-1})	k_{cat}/K_m ($\mu M^{-1}\cdot s^{-1}$)	K_m (μM)	k_{cat} (s^{-1})	k_{cat}/K_m ($\mu M^{-1}\cdot s^{-1}$)
AM	30 ± 2	54.0 ± 0.5	1.8 ± 0.1	3.13 ± 0.05	21.3 ± 0.3	6.8 ± 0.2	18 ± 1	53.0 ± 0.5	3.0 ± 0.2
CF[a]	9 ± 1	84 ± 2	9 ± 1	17 ± 1	0.96 ± 0.02	0.005 ± 0.006	12.7 ± 0.7	49.0 ± 0.8	3.9 ± 0.3
CRO[b]	28 ± 2	65 ± 1	2.4 ± 0.2	14.0 ± 0.7	0.61 ± 0.01	0.044 ± 0.003	51 ± 3	92 ± 3	1.8 ± 0.1
CAZ	126 ± 10	103 ± 4	0.82 ± 0.09	ND	ND	0.0085 ± 0.0002	105 ± 4	75 ± 1	0.71 ± 0.04
FDC	ND	ND	0.186 ± 0.005	ND	ND	0.00121 ± 0.00004	ND	ND	0.072 ± 0.002
FEP	19 ± 2	19.8 ± 0.7	1.1 ± 0.1	ND	ND	0.086 ± 0.002	40 ± 2	18.6 ± 0.6	0.47 ± 0.05
ATM[a]	1.20 ± 0.03	1.87 ± 0.08	1.57 ± 0.05	44 ± 7	5.106 ± 0.002	0.12 ± 0.02	2.4 ± 0.1	4.8 ± 0.6	1.98 ± 0.05
NCF[d]	12 ± 1	241 ± 7	20 ± 3	64 ± 6	689 ± 30	11 ± 2	32 ± 2	158 ± 3	5.0 ± 0.4

[a]K_m values were determined as K_i with nitrocefin as reporter substrate.
[b]Results for PER-2 are for cefotaxime.
[c]PER-2 kinetic parameters are from references 12 and 18.
[d]Nitrocefin hydrolysis parameters for PER-14 were calculated using the model for inhibition by substrate from Verlaine et al. (19). PER-14 T130G shows a competitive inhibition by product.
[e]AM, ampicillin; ATM, aztreonam; CAZ, ceftazidime; CF, cephalothin; CRO, ceftriaxone; FDC, cefiderocol; FEP, cefepime; NCF, nitrocefin; ND, not determined.

region, as observed in the crystallographic structure, and another in which the side chain is rotated by ~120°, orienting the hydroxyl group away from the binding pocket (Fig. 1A and B). In contrast, in PER-14, T130 rapidly adopted and maintained a rotated conformation in which the hydroxyl group points away from the active site (Fig. 1C and D), and the methyl group of T130 becomes oriented toward the region usually occupied by the sulfate group of DBOs. This conformational rearrangement is mechanistically relevant because residue 130 participates in the hydrogen-bonding and proton-transfer network required for efficient acylation by DBO inhibitors (14, 15). Therefore, the outward orientation of the T130 hydroxyl group, together with the placement of its methyl group toward the inhibitor-binding region, may perturb the optimal pre-acylation geometry without preventing substrate binding. The time evolution of the side-chain dihedral angle of residue 130 further supports this interpretation, showing that PER-14 remains in the rotated state, whereas PER-2 samples both conformations (Fig. S1).

Based on this observation, molecular docking calculations of AVI and REL were performed to evaluate how this local rearrangement affects inhibitor recognition by both PER-2 (for comparison) and PER-14. Overall, as observed in Fig. S2, the two inhibitors adopt productive poses oriented toward the catalytic S70 while engaging with key residues involved in substrate recognition and catalysis, including S/T130, R220, K234, T235, and T237 (through electrostatic/polar interaction with the sulfonate group), and with residues Q69, N132, E166, and H170 (by polar interaction with the amide/piperidin-4-yl carbamoyl group), which is consistent with a productive pre-acylation complex, as previously reported in the structure of PER-2 acylated by AVI (PDB 6D3G) (9). However, the PER-14 conformation with the outward-facing T130 hydroxyl group yielded less favorable docking solutions for both AVI and REL compared with the initial PER-14

TABLE 3 Inhibition kinetic parameters for PER-14 and PER-2 against AVI and REL[a]

Kinetic parameters	PER-14 (PER-2^{S130T})	PER-2[b]
AVI		
k_2/K ($M^{-1}\cdot s^{-1}$)	2.5 ± 0.2	2,200 ± 100
$K_{i\ app}$ (μM)	740 ± 40	20 ± 3
k_{off} (s^{-1})	ND	0.0004
REL		
k_2/K ($M^{-1}\cdot s^{-1}$)	3.5 ± 0.2	11,200 ± 600
$K_{i\ app}$ (μM)	10,000 ± 700	5.0 ± 0.6
k_{off} (s^{-1})	ND	0.0002

[a]ND, not determined (see text for details).
[b]AVI values from reference 9, REL values from reference 20.

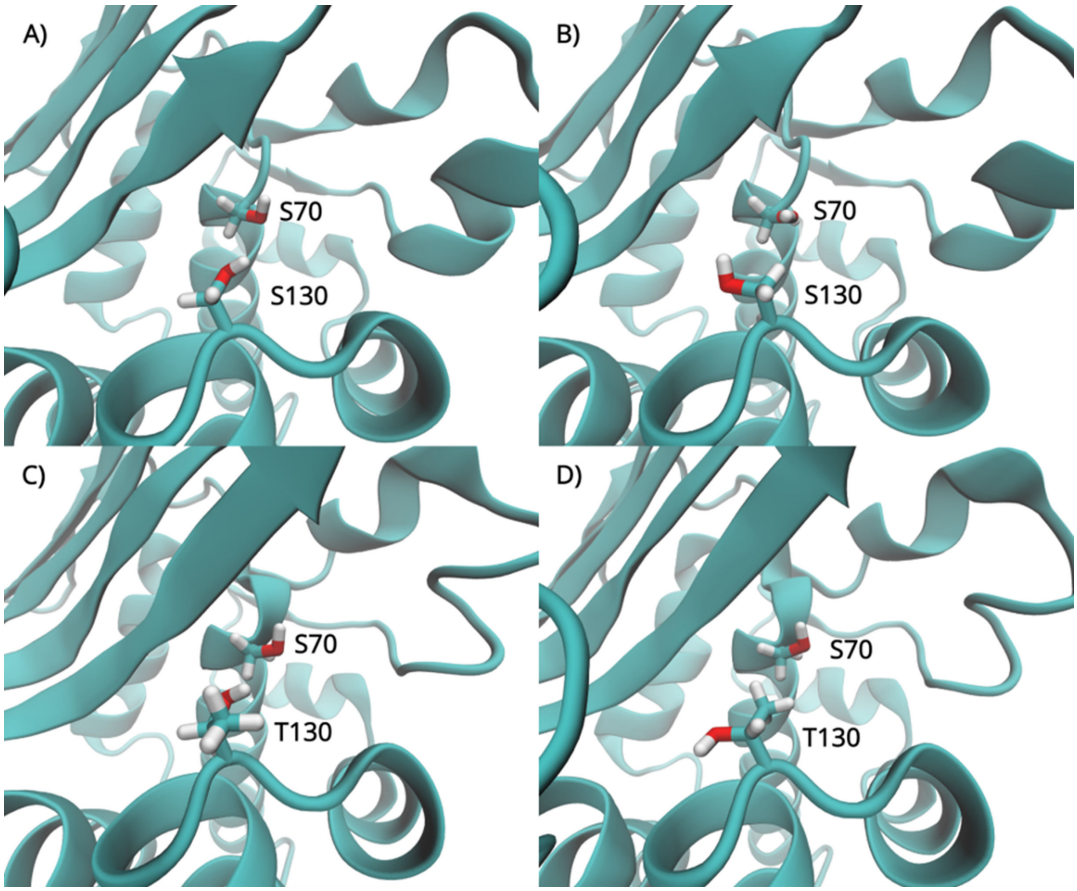

FIG 1 Representative orientations of residues 70 and 130 in PER-2 (A and B) and PER-14 (C and D) obtained from MD simulations.

structure, showing a 0.70 and 0.74 kcal/mol decrease in predicted binding energy and a 52% and 7% reduction in the population of the selected productive poses, respectively (Fig. S3).

To experimentally assess whether these structural differences affected avibactam trapping, intact-protein MALDI-TOF analyses were performed after incubation of PER variants with AVI (Text S2; Fig. S4). PER-2 rapidly formed an adduct-compatible species under equimolar conditions (1:1), detectable within 5 min and persisting throughout incubation. In contrast, PER-14 showed no detectable adduct accumulation under equimolar conditions and only exhibited an adduct-compatible mass shift after prolonged incubation under large inhibitor excess (1:50). These findings support impaired acyl-enzyme accumulation in PER-14 despite residual inhibitor recognition.

Together, these results support a model in which the S130T substitution does not abolish DBO binding but shifts the local conformational preferences toward less productive pre-acylation complexes. Although AVI and REL retain overall binding orientations toward the catalytic S70 in PER-14, the rotated T130 side chain and the altered local electrostatic environment reduce optimal inhibitor positioning for efficient acylation. These structural effects are modest at the docking level but are dramatically amplified kinetically, as reflected by the marked reductions in k_2/K and increases in $K_{i\ app}$, underscoring the critical role of precise ligand positioning in covalent inhibition of PER-type β-lactamases. In contrast, the S130G substitution likely causes a more severe disruption of the catalytic hydrogen-bonding network due to complete loss of the residue 130 side chain, consistent with the broader functional impairment observed for this mutant.

Consistent with observations in other class A β-lactamases, residue S130 plays a central role in DBO inhibition by acting as a proton donor during acylation (21, 22, 24) and contributing to the inhibitor's recyclization during deacylation (25). In PER-14, the additional methyl moiety of T130 likely reduces hydroxyl group flexibility compared to serine and introduces local steric constraints that impair productive inhibitor acylation while preserving β-lactamase hydrolysis. A mechanistic model is proposed in Fig. S5.

In this work, we demonstrate that PER-14 is resistant to inhibition by AVI and REL while retaining significant ESBL activity and the ability to hydrolyze FDC. Notably, $bla_{\text{PER-14}}$ differs from $bla_{\text{PER-2}}$ by a single nucleotide substitution, supporting the hypothesis that PER-14 evolved from PER-2 rather than arising from direct recruitment from *Pararheinheimera* spp. This is consistent with the stepwise accumulation of mutations that drive β-lactamase evolution, whereby limited genetic changes can result in advantageous amino acid substitutions. In this case, such evolution has led to a DBO inhibitor-resistant β-lactamase phenotype while preserving the ESBL profile of PER-2.

These features confer clear clinical relevance to PER-14, particularly in the context of the increasing use of FDC-, AVI-, and REL-based regimens as therapeutic options, which may favor its selection and therefore compromise the clinical efficacy of CAZ–AVI or ATM–AVI therapies.

ACKNOWLEDGMENTS

This research was partially funded by grants from the University of Buenos Aires (UBACyT 2023 20020220300115BA, awarded to P.P.), Agencia Nacional de Promoción Científica y Tecnológica (PICT-2021-I-A-00771, awarded to P.P., and PICT-2020-SERIEA-03730, awarded to M.R.), Consejo Nacional de Investigaciones Científicas y Técnicas (PIP 11220200100191CO, awarded to P.P., and PIBAA 2022-2023 N°28720210101143CO, awarded to M.R.), and project REPARA to D.M.M./S.I.D.

AUTHOR AFFILIATIONS

[1]Universidad de Buenos Aires, Facultad de Farmacia y Bioquímica, Instituto de Investigaciones en Bacteriología y Virología Molecular (IBaViM), Buenos Aires, Argentina
[2]Consejo Nacional de Investigaciones Científicas y Técnicas (CONICET), Buenos Aires, Argentina
[3]IQUIR (Instituto de Química Rosario), Consejo Nacional de Investigaciones Científicas y Técnicas (CONICET), Universidad Nacional de Rosario, Rosario, Argentina
[4]Facultad de Ciencias Bioquímicas y Farmacéuticas, Universidad Nacional de Rosario, Rosario, Argentina
[5]Medical Service, Louis Stokes Cleveland VA Medical Center, Cleveland, Ohio, USA
[6]GRECC, Louis Stokes Cleveland VA Medical Center, Cleveland, Ohio, USA
[7]Department of Medicine, Case Western Reserve University School of Medicine, Cleveland, Ohio, USA
[8]Department of Pharmacology, Case Western Reserve University School of Medicine, Cleveland, Ohio, USA
[9]Department of Molecular Biology and Microbiology, Case Western Reserve University School of Medicine, Cleveland, Ohio, USA
[10]Department of Biochemistry, Case Western Reserve University School of Medicine, Cleveland, Ohio, USA
[11]Department of Proteomics and Bioinformatics, Case Western Reserve University School of Medicine, Cleveland, Ohio, USA
[12]CWRU-Cleveland VAMC Center for Antimicrobial Resistance and Epidemiology (Case VA CARES), Cleveland, Ohio, USA

AUTHOR ORCIDs

Melina Ruggiero http://orcid.org/0009-0001-6744-9748
Robert A. Bonomo http://orcid.org/0000-0002-3299-894X

Gabriel Gutkind http://orcid.org/0000-0003-1999-9785
Diego M. Moreno http://orcid.org/0000-0001-5493-8537
Pablo Power http://orcid.org/0000-0002-7051-9954

FUNDING

Funder	Grant(s)	Author(s)
Consejo Nacional de Investigaciones Científicas y Técnicas	11220200100191CO	Pablo Power
Agencia Nacional de Promoción Científica y Tecnológica	PICT-2021-I-A-00771	Pablo Power
Universidad de Buenos Aires	20020220300115BA	Pablo Power
Consejo Nacional de Investigaciones Científicas y Técnicas	PIBAA 2022-2023 28720210101143CO	Melina Ruggiero
Agencia Nacional de Promoción Científica y Tecnológica	PICT-2020-SERIEA-03730	Melina Ruggiero

ADDITIONAL FILES

The following material is available online.

Supplemental Material

Supplemental material (AAC00378-26-s0001.docx). Fig. S1 to S5.

REFERENCES

1. Ebmeyer S, Kristiansson E, Larsson DGJ. 2019. PER extended-spectrum β-lactamases originate from *Pararheinheimera* spp. Int J Antimicrob Agents 53:158–164. https://doi.org/10.1016/j.ijantimicag.2018.10.019
2. Gutkind GO, Di Conza J, Power P, Radice M. 2013. β-lactamase-mediated resistance: a biochemical, epidemiological and genetic overview. Curr Pharm Des 19:164–208. https://doi.org/10.2174/13816128130202
3. Perez F, El Chakhtoura NG, Bonomo RA. 2025. Management of severe infections: multidrug-resistant and carbapenem-resistant Gram-negative bacteria. Med Clin North Am 109:735–747. https://doi.org/10.1016/j.mcna.2025.01.003
4. Estabrook M, Kazmierczak KM, Wise M, Arhin FF, Stone GG, Sahm DF. 2021. Molecular characterization of clinical isolates of Enterobacterales with elevated MIC values for aztreonam-avibactam from the INFORM global surveillance study, 2012-2017. J Glob Antimicrob Resist 24:316–320. https://doi.org/10.1016/j.jgar.2021.01.010
5. Poirel L, Ortiz de la Rosa J-M, Sadek M, Nordmann P. 2022. Impact of acquired broad-spectrum β-lactamases on susceptibility to cefiderocol and newly developed β-lactam/β-lactamase inhibitor combinations in *Escherichia coli* and *Pseudomonas aeruginosa*. Antimicrob Agents Chemother 66:e0003922. https://doi.org/10.1128/aac.00039-22
6. Soto KD, Alcalde-Rico M, Ugalde JA, Olivares-Pacheco J, Quiroz V, Brito B, Rivas LM, Munita JM, García PC, Wozniak A. 2024. Ceftazidime/avibactam resistance is associated with PER-3-producing ST309 lineage in Chilean clinical isolates of non-carbapenemase producing *Pseudomonas aeruginosa*. Front Cell Infect Microbiol 14:1410834. https://doi.org/10.3389/fcimb.2024.1410834
7. Li X, Zhou L, Lei T, Zhang X, Yao J, He J, Liu H, Cai H, Ji J, Zhu Y, Tu Y, Yu Y, Zhou H. 2024. Genomic epidemiology and ceftazidime-avibactam high-level resistance mechanisms of *Pseudomonas aeruginosa* in China from 2010 to 2022. Emerg Microbes Infect 13. https://doi.org/10.1080/22221751.2024.2324068
8. Ruggiero M, Papp-Wallace KM, Taracila MA, Mojica MF, Bethel CR, Rudin SD, Zeiser ET, Gutkind G, Bonomo RA, Power P. 2017. Exploring the landscape of diazabicyclooctane (DBO) inhibition: avibactam inactivation of PER-2 β-lactamase. Antimicrob Agents Chemother 61:1–11. https://doi.org/10.1128/AAC.02476-16
9. Ruggiero M, Papp-Wallace KM, Brunetti F, Barnes MD, Bonomo RA, Gutkind G, Klinke S, Power P. 2019. Structural insights into the inhibition of the extended-spectrum β-lactamase PER-2 by avibactam. Antimicrob Agents Chemother 63:1–12. https://doi.org/10.1128/AAC.00487-19
10. Liu X, Lei T, Yang Y, Zhang L, Liu H, Leptihn S, Yu Y, Hua X. 2022. Structural basis of PER-1-mediated cefiderocol resistance and synergistic inhibition of PER-1 by cefiderocol in combination with avibactam or durlobactam in *Acinetobacter baumannii*. Antimicrob Agents Chemother 66:e0082822. https://doi.org/10.1128/aac.00828-22
11. Mc Gann P, Geringer MR, Hall LR, Lebreton F, Markelz E, Kwak YI, Johnson S, Ong AC, Powell A, Tekle T, Bergman Y, Simner PJ, Bennett JW, Cybulski RJ, White BK. 2021. Pan-drug resistant *Providencia rettgeri* contributing to a fatal case of COVID-19. J Med Microbiol 70:001406. https://doi.org/10.1099/jmm.0.001406
12. Ruggiero M, Briceño Muñoz I, Gutkind G, Hujer AM, Bonomo RA, Power P. 2024. Insights into the activity of cefiderocol against PER-2 producing Enterobacterales. Antimicrob Agents Chemother 68:e0172023. https://doi.org/10.1128/aac.01720-23
13. Lahiri SD, Bradford PA, Nichols WW, Alm RA. 2016. Structural and sequence analysis of class A β-lactamases with respect to avibactam inhibition: impact of Ω-loop variations. J Antimicrob Chemother 71:2848–2855. https://doi.org/10.1093/jac/dkw248
14. Sun T, Bethel CR, Bonomo RA, Knox JR. 2004. Inhibitor-resistant class A beta-lactamases: consequences of the Ser130-to-Gly mutation seen in Apo and tazobactam structures of the SHV-1 variant. Biochemistry 43:14111–14117. https://doi.org/10.1021/bi0487903
15. Pemberton OA, Noor RE, Kumar M V V, Sanishvili R, Kemp MT, Kearns FL, Woodcock HL, Gelis I, Chen Y. 2020. Mechanism of proton transfer in class A β-lactamase catalysis and inhibition by avibactam. Proc Natl Acad Sci USA 117:5818–5825. https://doi.org/10.1073/pnas.1922203117
16. Heckman KL, Pease LR. 2007. Gene splicing and mutagenesis by PCR-driven overlap extension. Nat Protoc 2:924–932. https://doi.org/10.1038/nprot.2007.132
17. CLSI. 2025. Performance standards for antimicrobial susceptibility testing. 35th ed. CLSI Supplement M100. Clinical Laboratory Standards Institute.
18. Ruggiero M, Curto L, Brunetti F, Sauvage E, Galleni M, Power P, Gutkind G. 2017. Impact of mutations at Arg220 and Thr237 in PER-2 β-lactamase on conformation, activity, and susceptibility to inhibitors. Antimicrob Agents Chemother 61:e02193-16. https://doi.org/10.1128/AAC.02193-16

19. Verlaine O, Malempré R, Versées W, Matagne A, Frère J-M. 2024. Single time-point analysis of product and substrate inhibition. Sci Rep 14:23160. https://doi.org/10.1038/s41598-024-70805-9
20. Ruggiero M, Papp-Wallace KM, Brunetti F, Gutkind G, Klinke S, Bonomo RA, Power P. 2020. Arg220 and diazabicyclooctane (DBO) inhibitors: understanding structure activity relationships (SAR) in the PER β-lactamase, a unique class A enzyme. American Society for Microbiology, ASM Microbe 2020, USA.
21. Papp-Wallace KM, Winkler ML, Taracila MA, Bonomo RA. 2015. Variants of β-lactamase KPC-2 that are resistant to inhibition by avibactam. Antimicrob Agents Chemother 59:3710–3717. https://doi.org/10.1128/AAC.04406-14
22. Compain F, Dorchène D, Arthur M. 2018. Combination of amino acid substitutions leading to CTX-M-15-mediated resistance to the ceftazidime-avibactam combination. Antimicrob Agents Chemother 62:1–8. https://doi.org/10.1128/AAC.00357-18
23. Drusin SI, Le Terrier C, Poirel L, Bonomo RA, Vila AJ, Moreno DM. 2024. Structural basis of metallo-β-lactamase resistance to taniborbactam. Antimicrob Agents Chemother 68:e0116823. https://doi.org/10.1128/aac.01168-23
24. Winkler ML, Papp-Wallace KM, Taracila MA, Bonomo RA. 2015. Avibactam and inhibitor-resistant SHV β-lactamases. Antimicrob Agents Chemother 59:3700–3709. https://doi.org/10.1128/AAC.04405-14
25. King DT, King AM, Lal SM, Wright GD, Strynadka NCJ. 2015. Molecular mechanism of avibactam-mediated β-lactamase inhibition. ACS Infect Dis 1:175–184. https://doi.org/10.1021/acsinfecdis.5b00007